Statistical Vp-Vs relationships from well logs in Blackfoot

Yong Xu and John C. Bancroft

ABSTRACT

The statistical relationships between compressional wave velocity (V_P) and shear wave velocity (V_S) are evaluated from dipole logs of four wells in the Blackfoot area. The derived relationships from linear regression analysis are compared with Castagna's mud-rock line.

INTRODUCTION

A method was developed to look for the anomalies that deviate from the statistical relationship (Smith and Gidlow, 1987). In this method, the fluid factor is defined as

$$\Delta F = \frac{\Delta V_P}{V_P} - 1.16\frac{V_S}{V_P}\frac{\Delta V_S}{V_S} \qquad (1)$$

Derivation of equation (1) uses Castagna's mud-rock line that is a statistical relationship between V_P and V_S (Castagna, et. al., 1985) and defined as

$$V_P = 1.16V_S + 1360\,, \qquad (2)$$

where V_P and V_S are in m/sec.

Equation (2) is widely referred by many authors, however, it should be tested when it is applied to a local area. If a locally generated relationship between V_P and V_S with a similar form to equation (2) or with other forms exists in the survey, then the fluid factor or fluid stack will take advantage of this relationship.

In this paper, we analyze the dipole sonic logs that were collected in the Blackfoot area and attempt to evaluate the relationships between V_P and V_S.

STATISTICAL RELATIONSHIP BETWEEN V_P AND V_S

There are four wells with dipole sonic logs in the survey: 04-16, 08-08, 09-17, and 12-16. Figure 1 shows the location of wells including the four wells listed above. The map also shows the 3C-2D seismic line 950278 and the incised valley isopach. The wells investigated have different depth intervals for the dipole sonics. The 04-16 well has a dipole sonic from the top to the bottom, while the other three have dipoles in the zone of interest. The following table lists the top and bottom depths of the dipole logs of each well.

Table 1. The top depth and bottom depth of the dipole logs of the four wells, 04-16, 08-08, 09-17, and 12-16

Well name	Top (meters)	Bottom (meters)
04-16	135	1647
08-08	1362	1674
09-17	1440	1651
12-16	1229	1629

The compressional wave velocity, shear wave velocity, and bulk density are plotted respectively on Figures 2-5 for four wells. The formation tops are plotted on the well log curves. In this analysis, the samples to be used for each well are selected carefully. Each well has touched Mississippian carbonate, but the data below the Mississippian formation are not used in this analysis. Samples with extremely high or low velocity values are not used. For example, on Figure 3, at depth of 1600 meters, the V_P is extremely high, but the Vs is normal. This small portion is not reasonable to be used in the analysis. Consequently, the V_P value is limited to 1570 - 5000 m/sec and shear wave velocity is limited to 500 - 3500 m/sec.

Castagna's mud-rock line equation (2) fits a great variety of rocks very well. This is can be seen on Figure 6 which is adapted from the paper of Castagna et. al. (1985). In our analysis, only one trend line is attempted to be derived for the selected samples and no further analysis is done by differentiating lithology of the selected samples.

The cross-plots of V_P and V_S for the 04-16 well are shown on Figure 7 and 8. On Figure 7, all selected samples above the Mississippian formation are plotted, and the linear regression relationship is as the following equation:

$$V_{P_{04-16A}} = 1.30 V_{S_{04-16A}} + 1205 \qquad (3)$$

On Figure 8, the analysis is limited to the deep portion. The selected data above Mississippian and below 1000 meters is plotted and the linear relationship is found to be:

$$V_{P_{04-16B}} = 1.34 V_{S_{04-16B}} + 1150 \qquad (4)$$

The cross plots on Figure 7 and 8 for the 04-16 well show good linear relationships between V_P and V_S on both full logs and deep portion logs. However, the slope of the linear relationship for the deep portion is slightly larger than the slope obtained from full logs. The former is 1.34, and the latter is 1.30. The intercepts of both equations also are slightly different. The intercept of equation (3) is 1205, and that of equation (4) is 1150.

The Castagna's mud-rock line equation is plotted both on Figure 7 and 8. It can be seen that the selected samples with smaller value for V_P (2500m/s - 4000m/s) and smaller value for V_S (1000m/s - 2000m/s) fit mud-rock line fairly well and the samples with higher V_P and higher V_S are deviated from mud-rock line. Equation (3) fits mud-rock line better than equation (4). Because equation (4) is derived from the deep portion, we can say that the samples from the shallow portion (above 1000m) of the 04-16 well fit mud-rock line better than samples from the deeper portion.

Figure 9 cross-plots V_P versus Vs for the 08-08 well. The samples above the Mississipian formation, except the samples with very high P-velocity and the samples within coal layers, are plotted on the figure. On the 08-08 well, there is hydrocarbon indication on the Glauconitic channel zone from 1552.5m to 1595m. The V_P/V_S ratio is low over this portion. On Figure 8, the samples with low V_P/V_S on the Glauconitic channel zone are circled. The circled samples are separated from other samples on the V_P-V_S cross-plot. The trend-line for all selected samples is plotted on this figure, and its equation is

$$V_{P_{08-08}} = 0.95V_{S_{08-08}} + 1915. \qquad (5)$$

This equation has smaller slope and higher intercept than Castagna's mud-rock line that is drawn on Figure 9. Due to the samples on the channel zone, equation (5) does not reflect the trend of the samples that fall outside of the Glauconitic channel zone. The mud-rock line does not reflect the V_P-V_S relationship for the samples that fall outside of the Glauconitic channel zone.

Figure 10 shows the V_P-V_S cross plot and the fitted trend line for the 09-17 well. The samples show a linear trend on the figure. The equation for the trend is

$$V_{P_{09-17}} = 1.74V_{S_{09-17}} + 272. \qquad (6)$$

Equation (6) has a bigger slope than Castagna's mud-rock line equation, and has a much smaller intercept. It can be seen that the mud-rock line is not as good as equation (6) to show the trend of the selected samples on Figure 10.

Figure 11 shows the V_P-V_S relationship for the 12-16 well. The statistical relationship is

$$V_{P_{12-16}} = 0.97V_{S_{12-16}} + 1915. \qquad (7)$$

On Figure 11, the samples show a linear trend between V_P and V_S. The slope of equation (7) is smaller than the slope of mud-rock line. And the intercept of equation (7) is bigger than that of mud-rock line equation. The mud-rock line equation is also drawn on this figure. It can be seen that most of the selected samples fall above the mud-rock line.

All V_P-V_S samples from the four wells are cross-plotted on Figure 12. The linear relationship is

$$V_{P_{all}} = 1.26 V_{S_{all}} + 1282 . \quad (8)$$

Compared with equations (4)-(7), the slope and the intercept of equation (8) are closer to the slope and the intercept of mud-rock line equation. This suggests that the population for statistical analysis in the 08-08, 09-17, and 12-16 wells is too small, and a larger population is needed to compare to the mud-rock equation. However, on Figure 12, many samples with higher V_P (V_P > 3300m/s) and higher V_S (V_S > 1700m/s) deviate from the mud-rock line.

CONCLUSIONS

The statistical relationships between V_P and V_S were obtained by linear regression analysis of four wells with dipole sonic logs in the Blackfoot field. The relationships are compared with Castagna's mud-rock equation. The 04-16 well shows good linear relationships between V_P and V_S. Samples on the reservoir channel zone on the 08-08 well show a large deviation from the statistical trend. Three wells, 08-08, 09-17, and 12-16, were edited to eliminate abnormal portions and they show different fitted trends from each other and from the 04-16 well. These differences may reflect the subsurface lithology changes and poorly sampled populations. The available log portion lengths and the data quality may also affect the fitted trends and cause the statistical trend differences. To obtain a reliable relationship between V_P and V_S, more careful interpretation of the well logs and more wells where longer dipole sonics exist are required. All derived trend lines for each well have differences from Castagna's mud-rock line equation. It is observed from the large population analysis of the 04-16 well that the samples with lower velocity fit Castagna's mud-rock line better and the samples with higher velocity deviate from mud-rock line.

ACKNOWLEDGMENTS

We would like to thank the sponsors of CREWES Project. We would also like to thank Colin Potter for his suggestions and corrections for the paper.

REFERENCES

Castagna, J. P., Batzle, M. L. and Eastwood, R. L., 1985, Relationship between compressional wave and shear wave velocities in clastic silicate rocks: Geophysics, V. 50, 571 - 581.

Miller, S. L. M., Aydemir, E. O., and Margrave, G. F., 1995, Preliminary interpretation of P-P and P-S seismic data from the Blackfoot broad-band survey: CREWES Research Report 1995, Chapter 42.

Smith, G. C., and Gidlow, P. M., 1987, Weighted stacking from rock property estimation and detection of gas: Geophys. Prosp. 35, 993-1014.

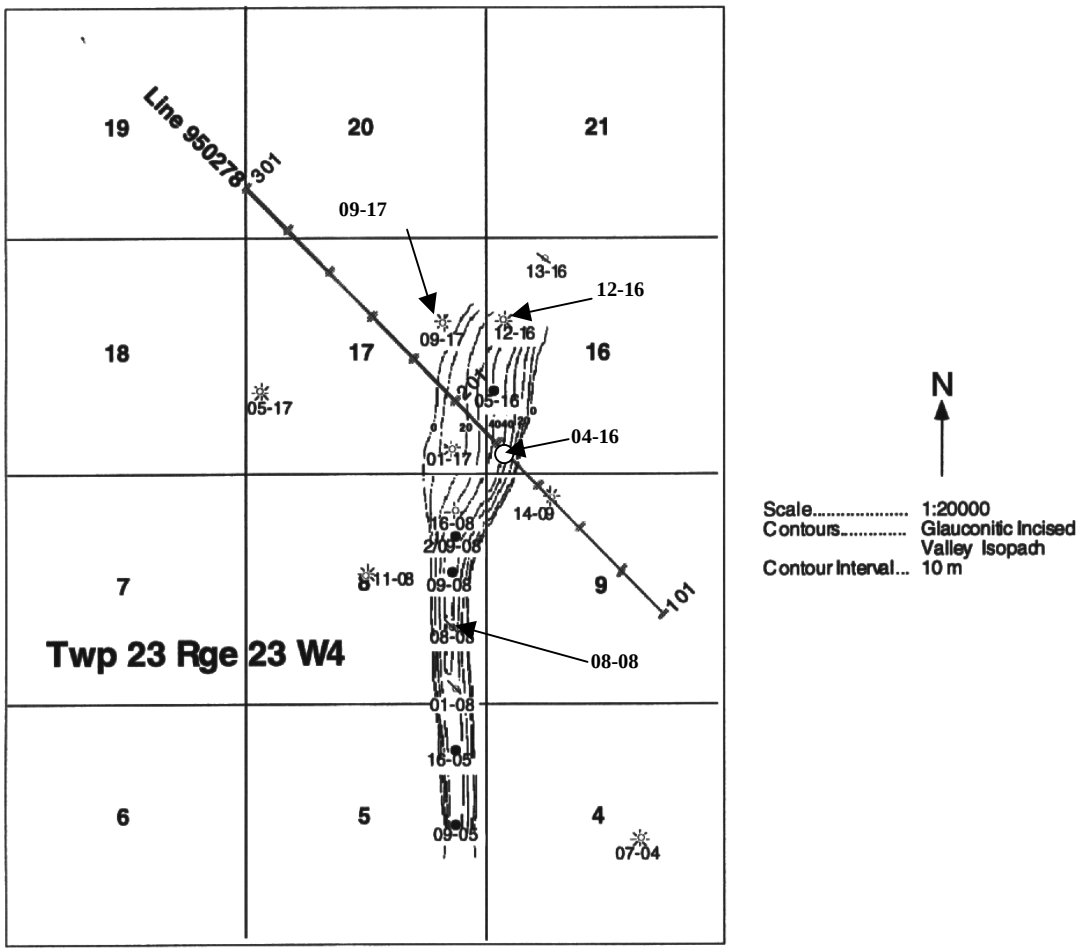

Figure 1. Location map of 3C-2D seismic line 950278, well control and the incised valley isopach (Miller et. al., 1995)

Contents

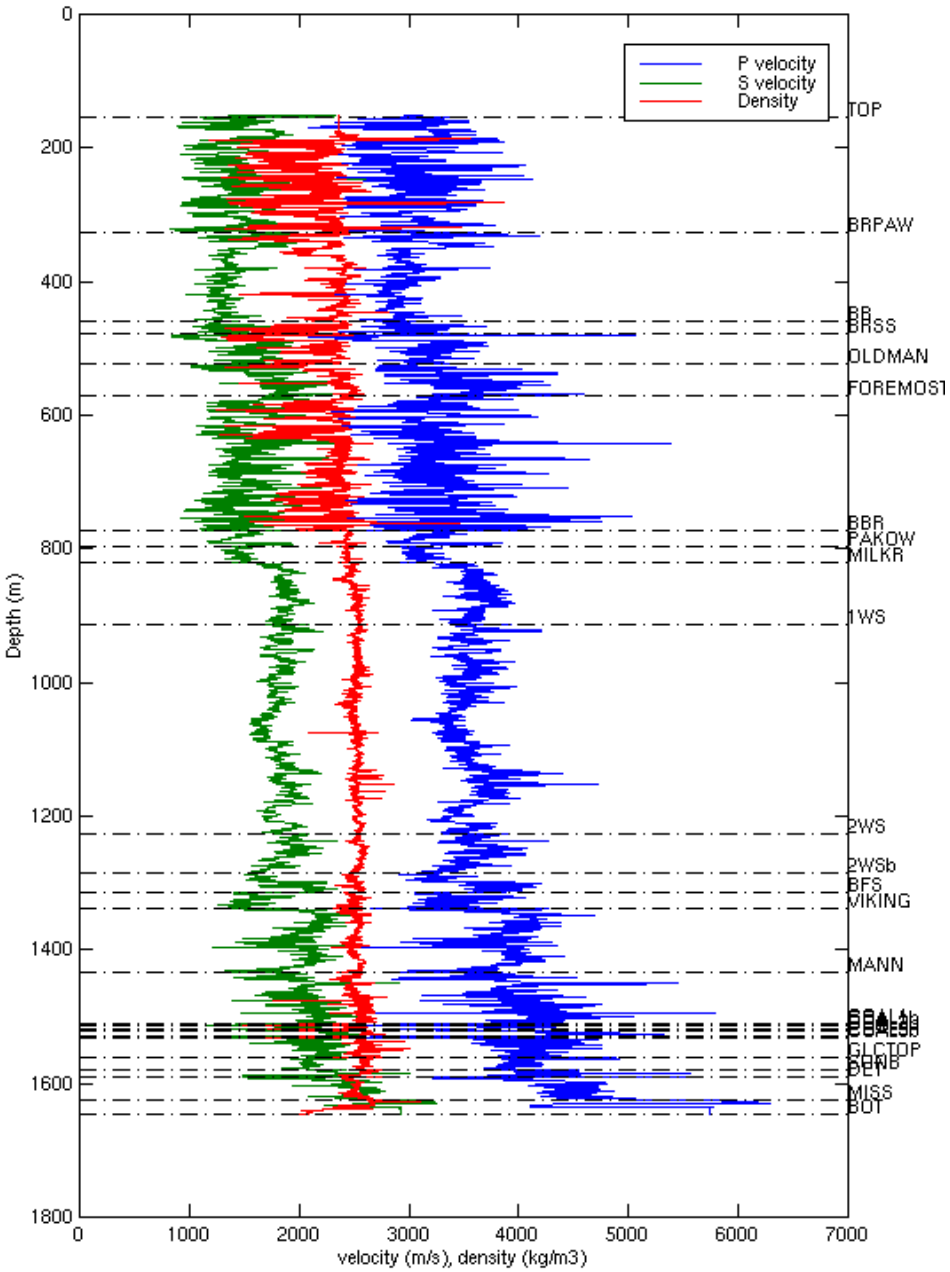

Figure 2. Log curves of well 04-16 and formation tops

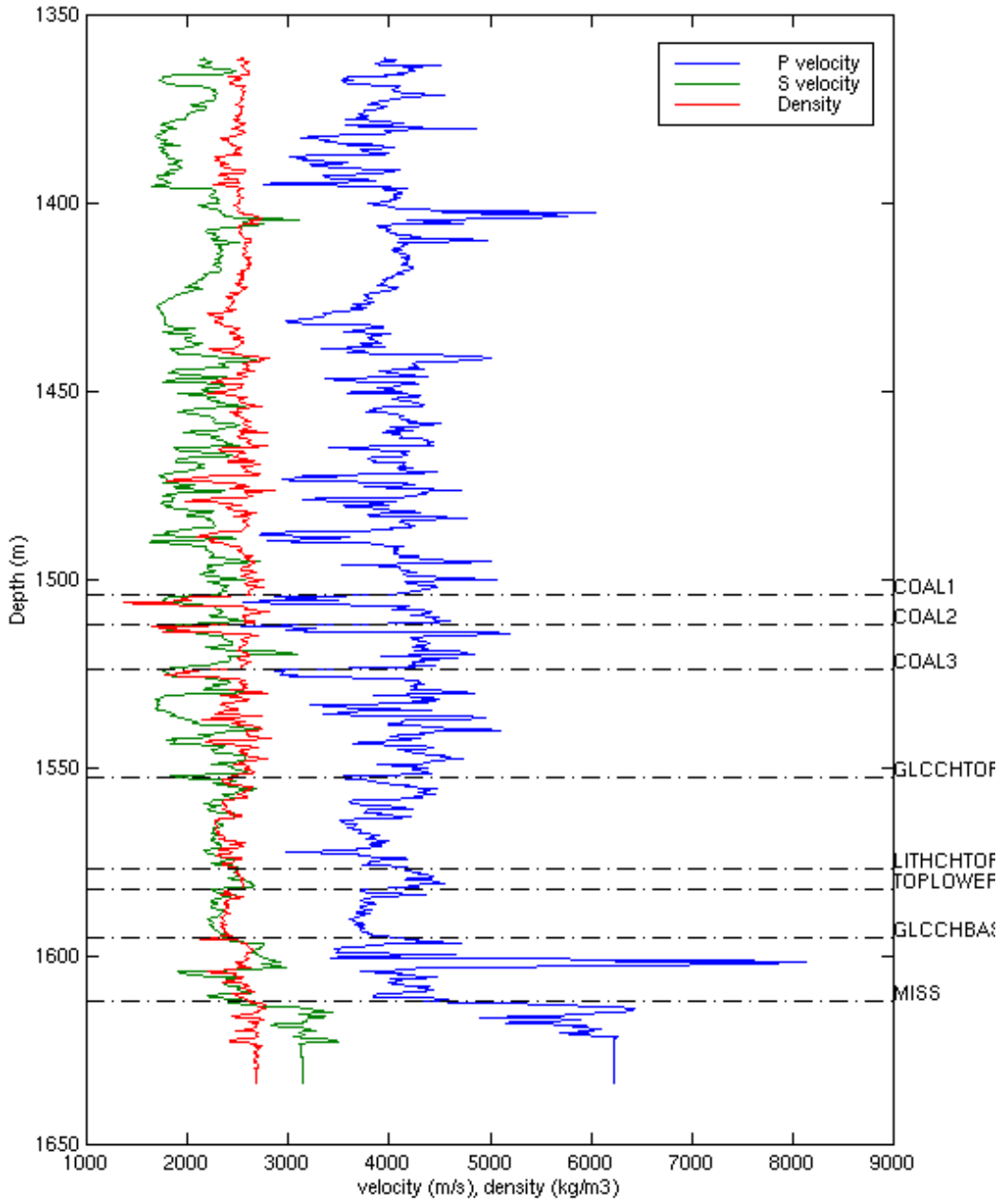

Figure 3. Log curves of well 08-08 and the formation tops

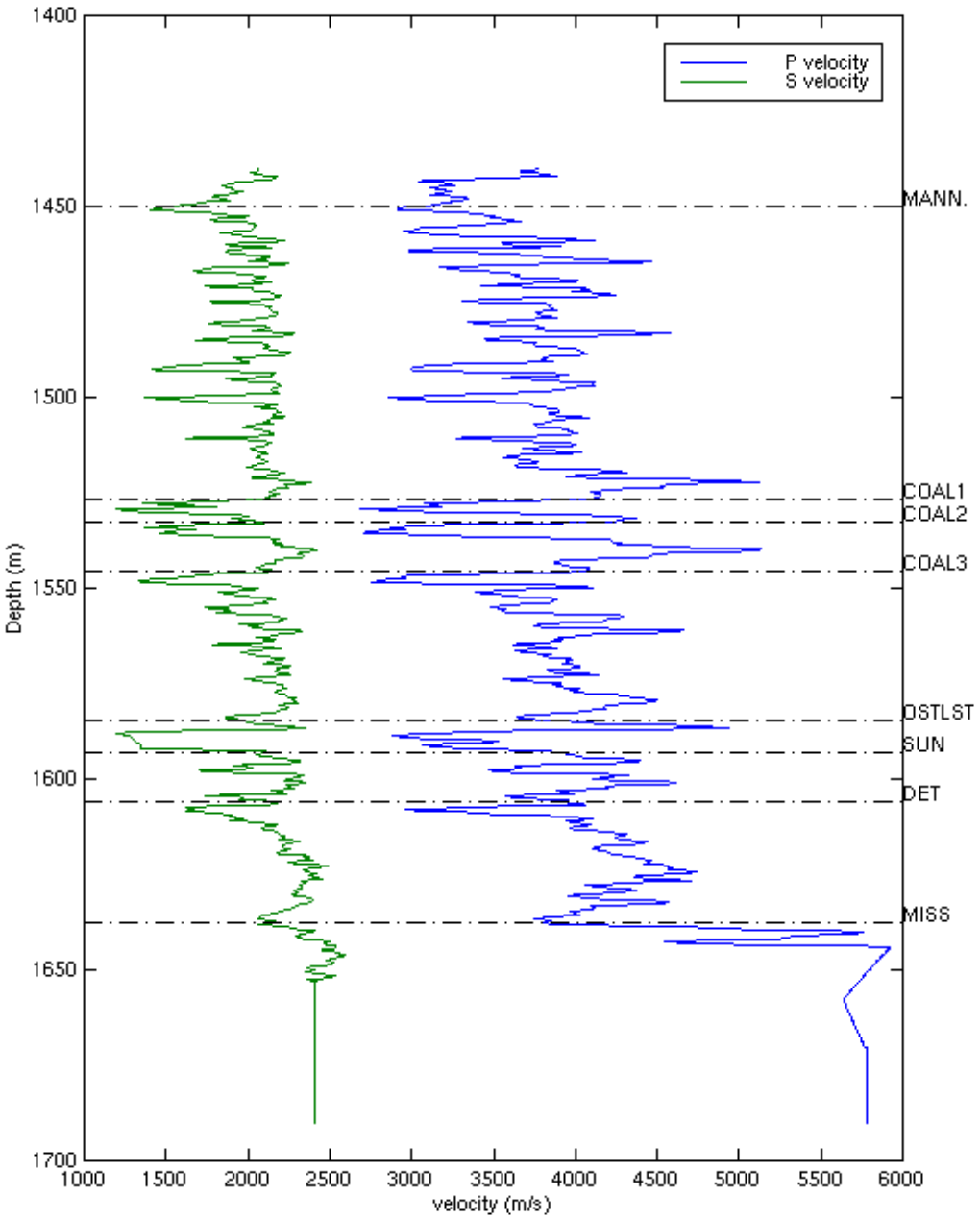

Figure 4. Log curves of well 09-17 and formation tops

Contents

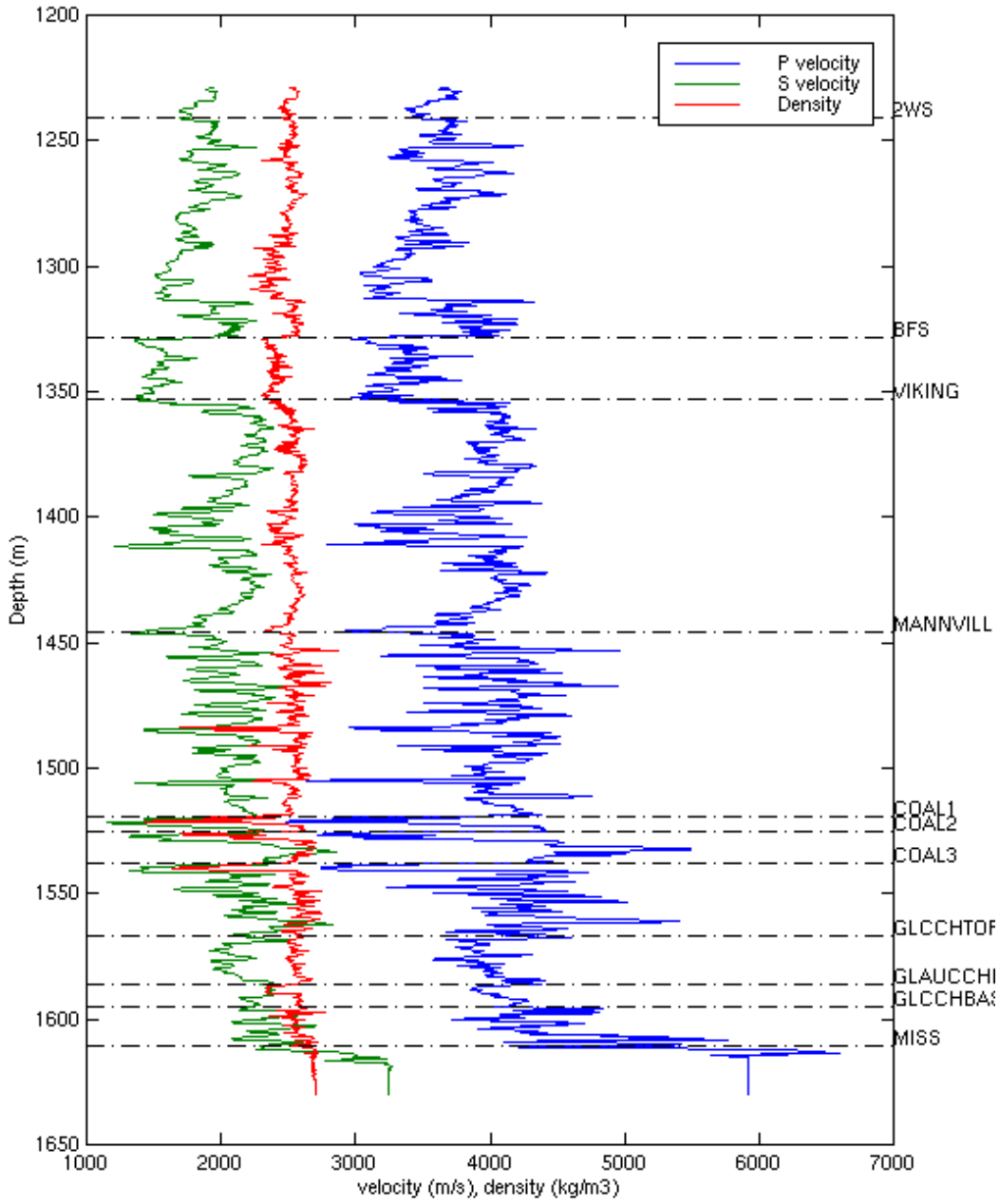

Figure 5. Log curves of well 12-16 and formation tops

Contents

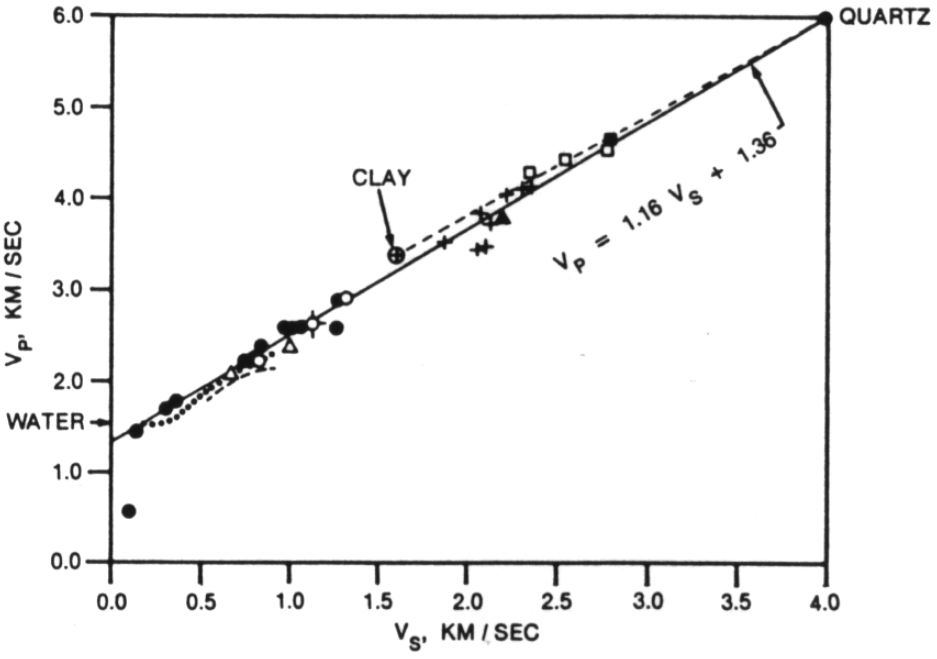

■ KOERPERICH, 1979, SILTSTONE, SONIC LOG (15 KHz)
□ EASTWOOD AND CASTAGNA, 1983, WOLFCAMP SHALE, SONIC LOG (10 KHz)
▲ OIL SHALE, SONIC LOG, (25 KHz)
\+ LINGLE AND JONES, 1977, DEVONIAN SHALE, SONIC LOG
⊹ HAMILTON, 1979, PIERRE SHALE
○ HAMILTON, 1979, GRAYSON SHALE
⊛ HAMILTON, 1979, JAPANESE SHALE
● LASH, 1980, GULF COAST SEDIMENTS, VERTICAL SEISMIC PROFILE
△ SHALE, SONIC LOG, INVERTED STONELEY WAVE VELOCITIES, (1 KHz)
•••• HAMILTON, 1979, MUDSTONES
– – – EBENIRO, 1981, GULF COAST SEDIMENTS, SURFACE WAVE INVERSION
⊕ TOSAYA'S "CLAY" POINT (EXTRAPOLATION FROM LABORATORY DATA)

Figure 6. Compressional and shear wave velocities for mud-rocks from in-situ sonic and field seismic measurements (Castagna et. al., 1985)

Contents

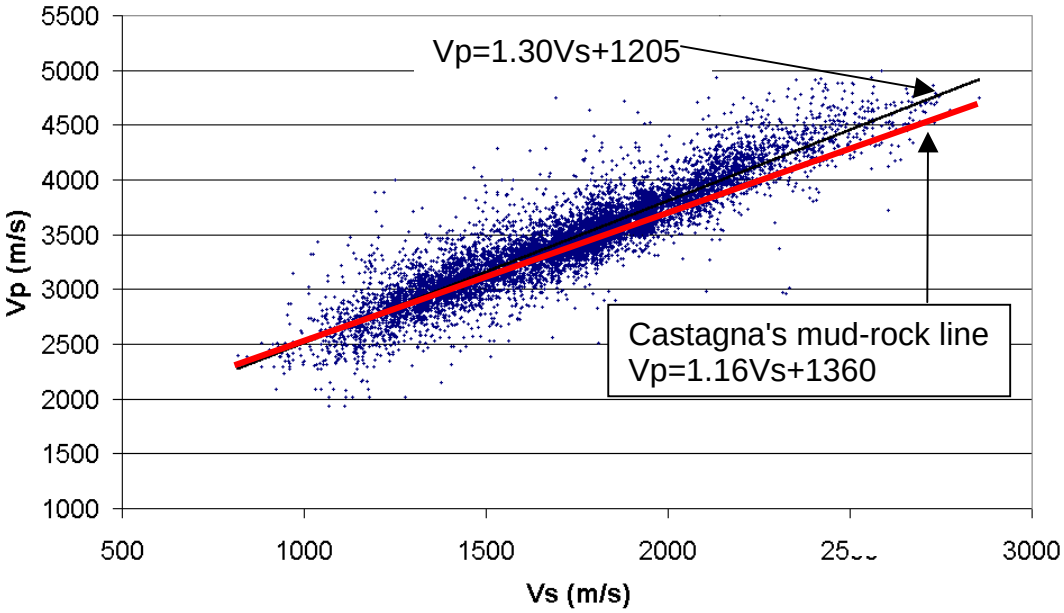

Figure 7. Cross-plot of Vp and Vs of well 04-16 (all data above Mississippian formation)

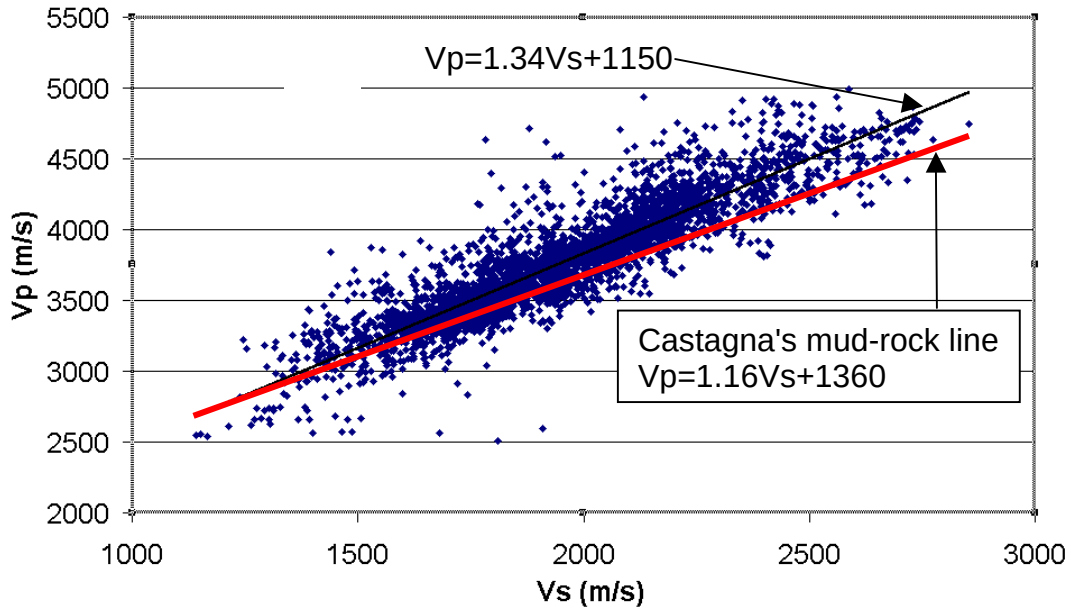

Figure 8. Cross-plot of Vp and Vs of well 04-16 (portion below 1000 meters and above Mississippian formation)

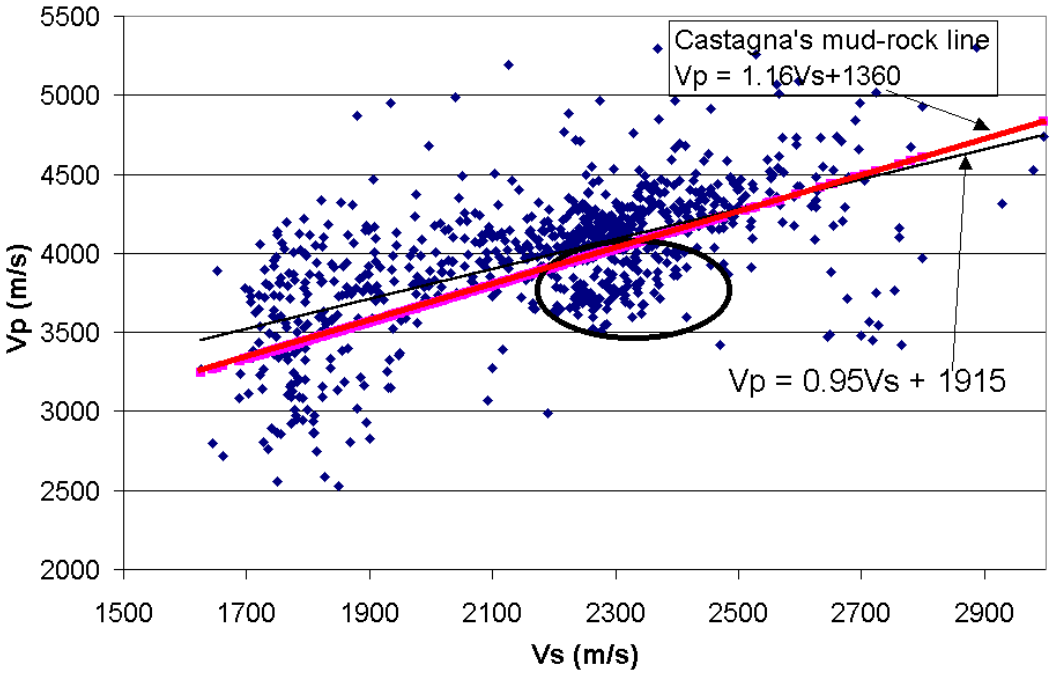

Figure 9. Cross-plot of Vp and Vs of well 08-08 (portion below 1000 meters and above Mississippian formation)

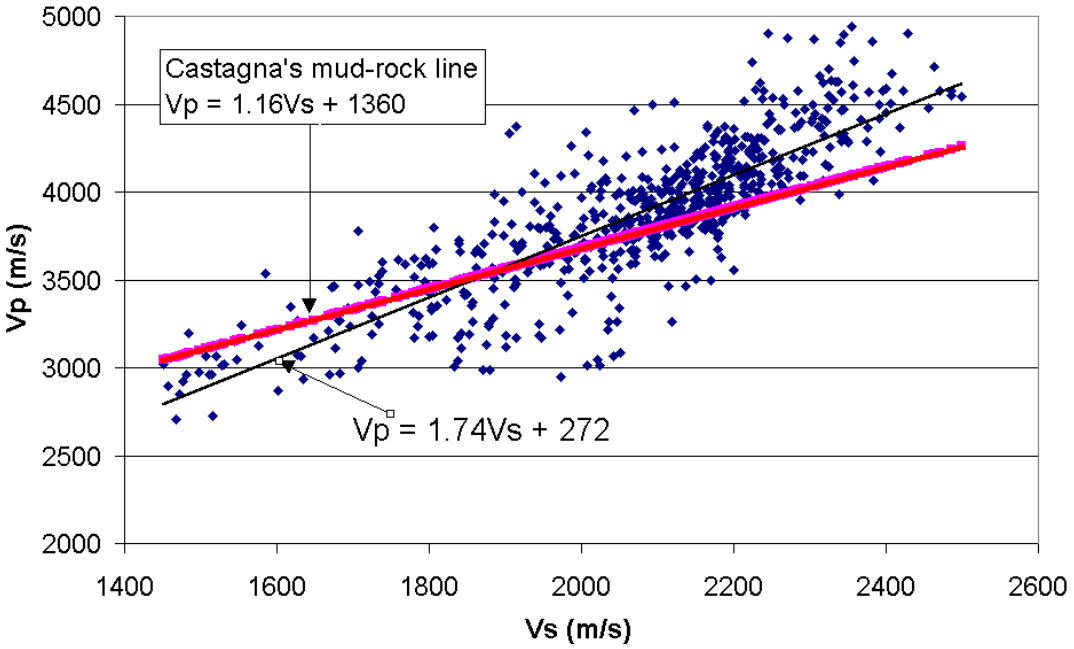

Figure 10. Cross-plot of Vp and Vs of well 09-17 (above Mississippian formation)

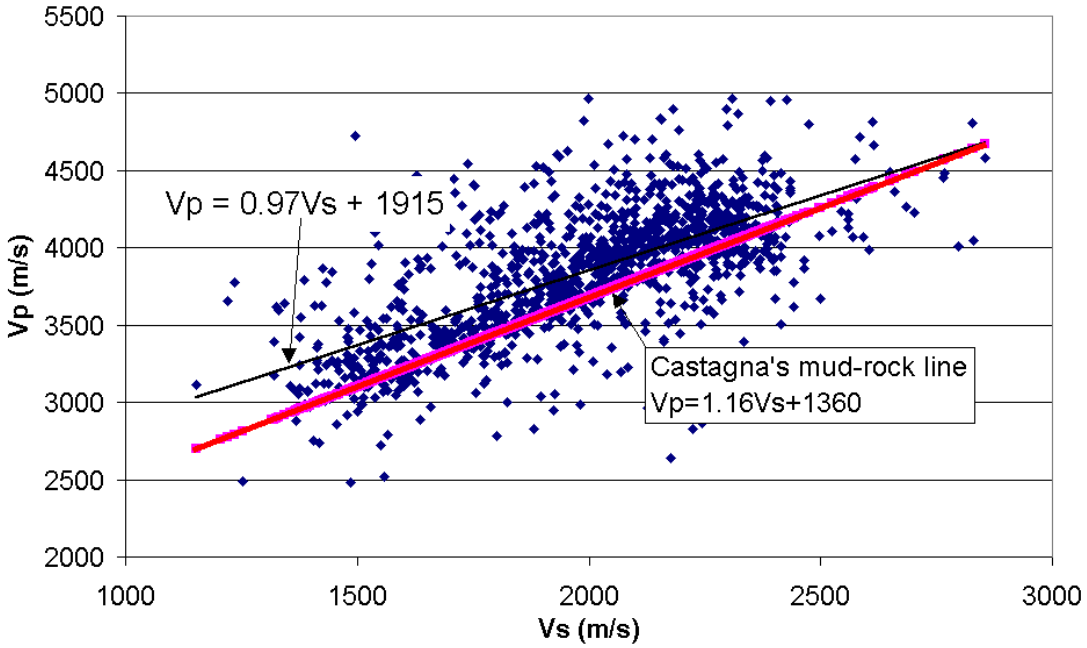

Figure 11. Cross-plot of Vp and Vs of well 12-16 (portion above Mississippian formation)

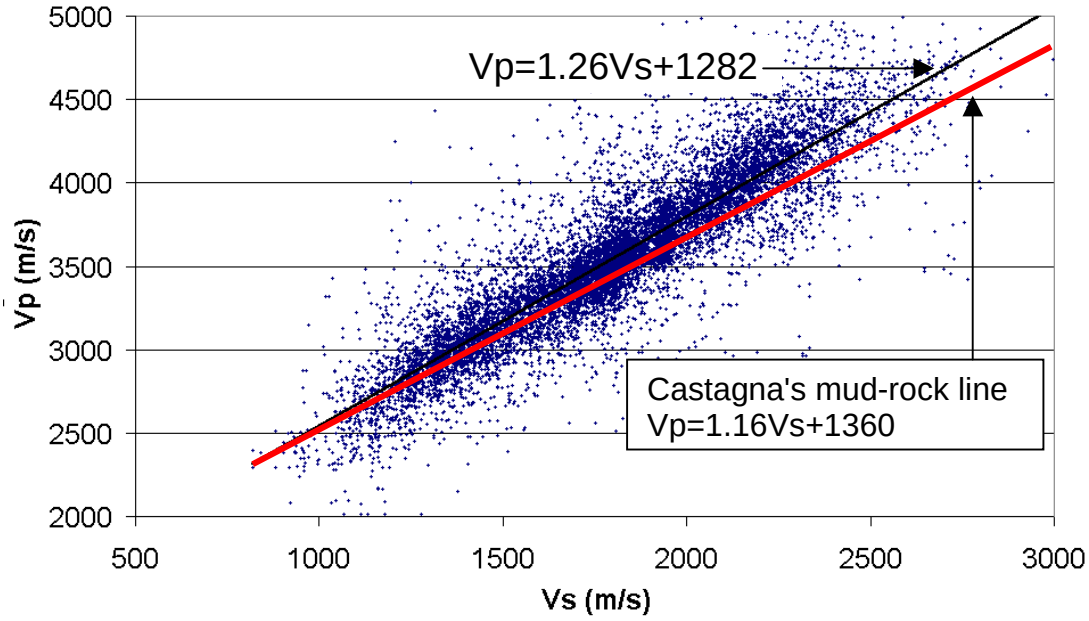

Figure 12. Cross-plot of Vp and Vs of four wells (portion above Mississippian formation)